A Foundry Fabricated Surface-micromachined High-speed Rotation Sensor Using Wireless Transmission

Winston Sun[1], Tao Mei[2], and Wen J. Li[1],*

[1]*Department of Mechanical and Automation Engineering, The Chinese University of Hong Kong*
[2]*State Key Laboratories of Transducer Technology, Institute of Intelligent Machines, Chinese Academy of Sciences*

ABSTRACT

A novel MEMS surface-micromachined non-contact high-speed rotation sensor with total surface area under 4mm^2 is now under development. Various versions of the sensor have been designed and were fabricated using the MCNC Multi-User MEMS Processes (MUMPs). This paper reports the initial characterization of the sensor and presents the results of transmitting the sensor data via a commercial wireless transmission chip. Initial results indicate that this piezoresistive sensor is capable of measuring rotation speeds from 1000 to 4000 rpm with linear output. The responsivity of the sensor is 3Hz/rpm in this region.

Subject Areas: *Silicon devices and technology, sensors and actuators.*

1. INTRODUCTION

Tachometers have been widely used to measure the angular speeds of rotating objects. In general, contact mechanical-based tachometers, although capable of giving measurements conveniently, are less accurate than AC or DC electromagnetic-based tachometers. Nevertheless, each type has its own advantages and shortcomings depending on the applications [1,2]. Optical tachometers are also available that give relatively accurate readings with wide rpm range [3,4]. However, Kwa et al. [5] pointed out that some optical sensors are quite sensitive to background light and contamination.

Recently, many new sensor devices based on different principles, including non-contact magnetic field [6], Faraday induction [7], and capacitive [8], have been built. These techniques, however, impose restrictions on the material properties or geometry of the rotational components to be measured, and they also limit the effective measurable rotation speed. In addition, all these sensors must be accompanied with a stationary reference, which is externally mounted to the systems' housing for proper operation. Imagine a mechanical transmission system or a gearbox assembly with lots of gears. If for diagnostic purpose the angular speed of each individual gear is to be measured, then traditional tachometers might not be a good solution.

We propose to build a MEMS rotation sensor that can be potentially integrated with wireless-transmission electrical circuitry. Since these micromachined sensors will be small, they can be directly embedded into the rotating objects such as gears or shafts, hence no sensor reference mounting is needed. Many MEMS rotation sensors have been fabricated using piezoelectric, piezoresistive, or capacitive principles [9,10,11]. However, the existing sensors are designed mainly for low angular speed and acceleration measurements. In addition, to the best of our knowledge, no high-speed rotations sensors were built using the MCNC commercial foundry service and have wireless transmitted output.

This paper presents the design, analysis, and initial experimental results of the polysilicon cantilever beam rotation sensors which can measure angular speeds between 1000 to 4000 rpm. These sensors are designed to have small size, low power consumption, low cost, wide dynamic range, and yet accurate. For demonstration, we have selected to use the MCNC MUMPS foundry to fabricate the mechanical elements which were then interfaced with commercial wireless transmission chips.

2. SENSOR CONCEPT AND DESIGN

The concept for measuring rotation of a spinning body using embedded micro-sensors is illustrated in Figure 1. A three dimensional illustration of a sensor is shown in Figure 2. We have used the MCNC MUMPs process to fabricate the sensor shown in this figure. The oxide layer underneath the mass platform was sacrificially released using hydrofluoric acid and critical CO_2 drying process. Etch holes were needed to provide shorter release etch paths under large features like the mass platform, which is supported only by two polysilicon cantilever beams and therefore is free for deflection by centrifugal forces. Scanning electron microscope (SEM) picture of a pair of the surface-micromachine sensors is shown in Figure 3.
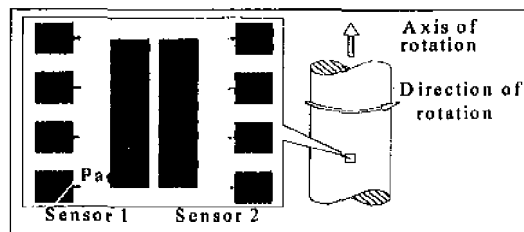

Figure 1. Conceptual drawing of micro-sensors embedded in rotating structures to measure rotation (not to scale).

Corresponding address: The Chinese University of Hong Kong, Department of Mechanical and Automation Engineering, MMW 425, Shatin, NT, Hong Kong. Email: wen@mae.cuhk.edu.hk.
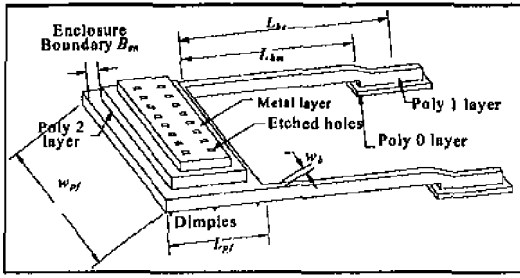
72

Figure 2. Three dimensional drawing of a surface-micromachined rotation sensor using polysilicon as cantilever beams supporting a multi-layered mass platform).
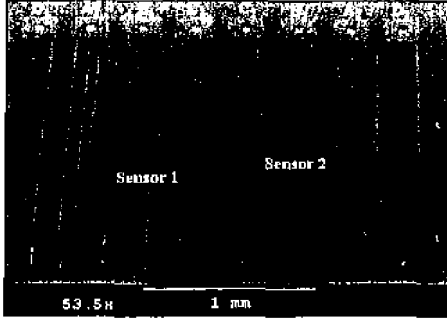

Figure 3. SEM picture of a pair of fabricated sensors. The curvature of the mass plate is due to residual stress between different layers of materials making up the plate.

2.1 Theoretical Analysis

As shown in Figure 4, a set containing two identical sensors in opposite direction is oriented so that the axes of the cantilever beams are perpendicular to the axis of rotation. As will be discussed later, a set of 2 sensors is needed to measure the angular acceleration of the rotating element. If no linear motion along the rotation axis then lateral deflection of the beams, or transverse stress, can be neglected. Excluding the substrate, a MCNC fabricated sensor is less than $5.1\mu m$ thick (platform) and weighs about $15\mu g$. The side view of a stationary sensor is illustrated in Figure 5. As shown, the initial moment arm from the centroid c to the fixed end F is a constant. When a centrifugal force is induced on the seismic mass by an angular velocity (ω) or acceleration (α), the length of this moment arm will change. From Figure 4 we can observe that the transverse load $P = m \cdot r \cdot \omega^2$ induced by rotation and the axial load $N = m \cdot r \cdot \alpha$ caused by angular acceleration (r is the distance from the axis of rotation to the seismic mass) both act on the centroid c of the platform. The distance e_c is a constant depending on the number of polysilicon layers. It is measured from the centroid of the platform to the neutral axis of the beam. The maximum strain on the cantilever beams occurs at F, the fixed end of the beams. From Fan et al. [12] the maximum allowable strain of polysilicon is about 1.7%. At $t > 0$ sec, the platform will be raised by a distance h_{cg} due to centrifugal force. Consequently the beams will be under stress and deformed in a curved shape. The beams will also undergo slight elongation or shortening depending on the combined effect of P and N. The moment

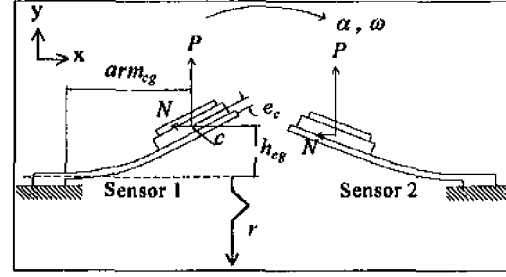arm measured from the fixed end to the centroid will also be shifted from initial distance to arm_{cg}.

Figure 4. Illustration showing a pair of rotation sensors. The design parameters are shown in this figure.
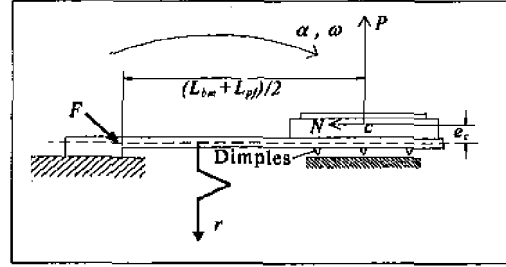

Figure 5. Illustration of the sideview of a rotation sensor. The dimples are used to prevent stiction of the platform to the substrate surface, which is a dominant phenomenon in surface-micromachined structures.

The governing differential equation for the bending beam is shown in Equation 1 below. The moment and stress equations are shown in Equations 2 and 3, respectively.

$$EI\frac{d^2 y_i}{dx_i^2} + P \cdot x \pm N \cdot y - M_i = 0 \tag{1}$$

$$M_i = P \cdot arm_{cg} \pm N \cdot h_{cg} \tag{2}$$

$$\sigma_i = M_i \cdot (t_{bm}/2)/I_{bm} \mp N/A_{bm} , i = 1, 2 \tag{3}$$

The index i denotes sensors 1 and 2 in Figure 4. In Equation 3 I_{bm} is the moment of inertia of the cross-section area about the neutral axis. $A_{bm} = t_{bm} \cdot (2 \cdot w_{bm})$ is the total cross-section area of the two beams. Equation 1 is obtained by summing the moments about any arbitrary point (x_i, y_i) along the beam i. Analytical solutions of Equation 1 can be readily obtained from symbolic mathematical packages (i.e., Mathematica) for a given set of values of r, ω and α. For transient calculations, the results of Equation 1 can be used to obtain arm_{cg} and h_{cg} at a given time, which can then be used in Equation 2 to obtain a more accurate solution.

The deflection or elongation of the beams causes a change of resistance of the polysilicon, which can be converted into a measurable change of voltage by connecting the sensors in a Wheatstone-bridge configuration [13]. The change of resistance due to beam elongation can be expressed as a function of gauge factor G or in terms of the piezoresistance coefficient π_{44} [14]. This is shown in Equation 4:

$$\frac{\Delta R_i}{R} = \frac{G}{L_{bm}} \cdot \int_0^{L_{bm}} \frac{\sigma_i}{E} dx = \frac{\pi_{44}}{2} \cdot (\sigma_{ll} - \sigma_{tl}) \tag{4}$$

73

where R is the total resistance of the sensor and for polysilicon is typically about 10 $\Omega/\square$ [15]. π_{44} is taken to be 138.1×10^{-11} Pa^{-1}, a result published by Smith [16] and verified by Beaty et al. [17]. σ_l is the longitudinal stress in Equation 1, and σ_t is the transverse stress which can be neglected at steady state conditions. When a steady state rotational speed is achieved, axial load N tends to zero. The two sensors will have the same deflection and change of resistance. However, when the angular acceleration α is $>>$ 0, such as during motor startup or under sudden change of speed, the transient response of Sensor 1 and Sensor 2 will be different due to the contribution from N. Hence, by monitoring the transient response of the sensors, the direction of acceleration can be determined. We have used the above theoretical analysis in designing the sensors to measure angular speeds ranging from 1000 to 4000 rpm.

3. EXPERIMENTAL RESULTS

Each MCNC run gave us 14 chips that have 10 rotation sensors and other devices designed for our various on-going projects. We have measured the change of resistance due to bending of the piezoresistive polysilicon cantilever beams for sensors of different designed parameters on different MCNC chips. Table 1 below is a representative comparison of two sensors with different cantilever beam width (W). In the table, f denotes failure of the beams due to excessive strain at the given deflection angle. The deflection angle is the angle between the tip of the mass platform and the substrate. The resistance change typically varies from 0.5 to 1% as shown in the table.

platform size: 600x320				
defl. angle	W=30μm, R_{3o}: 154.9Ω		W=14μm, R_{3o}: 266.75Ω	
	$\Delta R_{3\,(Ohms)}$	%	$\Delta R_{3\,(Ohms)}$	%
25	0.474	0.306	1.364	0.511
35	0.852	0.550	2.687	1.007
45	1.292	0.834	3.963	1.486
55	f	f	5.486	2.057

Table 1. Representative comparison of resistive change due to supporting beam bending for different structural designs.

Figure 6 is a conceptual drawing of the test setup for measuring the rotation speed of a disk wirelessly using the fabricated sensors. In our design the rotating disk is replaceable. Another sensor set with the same beam and platform dimensions is placed in the other side of the rotating disk as shown in the figure and used as reference sensors. The seismic mass and cantilever beams of these sensors are anchored to the nitride layer such that no stress is induced on the beam by centrifugal forces. The power supply, and the wireless data transmission chips are placed within a small package made by a CNC plastic injection machine, which is then placed on the rotating disk.

Commercial wireless transmitters and receivers which can be eventually interfaced with the MEMS sensors were evaluated for signal transmission. The

change of resistance across the bending beams (ΔR_3) is transduced into a change of differential voltage and then amplified by the AD620 instrumentation amplifier, which has an adjustable gain between 1 and 1000. The amplified voltage is then converted into frequency signal by an AD654 voltage to frequency converter. This stage is essential for the Radiometrix TX2 transmitter to provide stable signal transmission. The potentiometer at R_4 should be adjusted such that variation of bridge output is beyond the initial offset and within the linear region of AD620 as well as bounded by the upper frequency limit of TX2 at around 28 kHz. The signal is detected wirelessly by the Radiometix RX2 (not shown in the figure). A schematic drawing of the circuit system is shown in Figure 7.
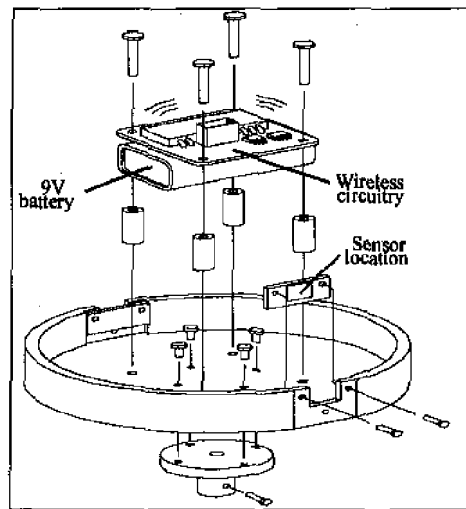

Figure 6. Conceptual drawing of the experimental rotating disk packaged with wireless rotation MEMS sensors.
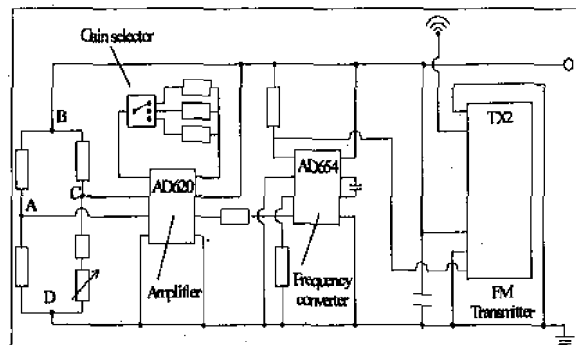

Figure 7. Schematic drawing of the transmition circuit system.

The circuit shown above was calibrated using a potentiometer that has a nominal value close to R_3 (resistance of a designed sensor). The frequency output of the AD654 versus the change of the potentiometer (R_4) is shown in Figure 8. Note a 20% change of resistance gives a linear output frequency between 10 to 25 KHz. Each moving-platform sensor was designed to have three integrated piezoresistors on chip to form a Wheatstone-bridge. The bridge output was connected to the AD620 (as shown in Figure 7) by wirebonding. We have observed linear

output of the receiver frequency versus rotation speed when the sensor is packaged on the 5cm disk using the method described in Figure 6. Typical frequency output received by the RX2 receiver is shown in Figure 9. The sensor tested in this case has a 600X320μm platform supported 30μm wide, 200μm long beams. The MCNC polysilicon beams are typically about 3μm thick.
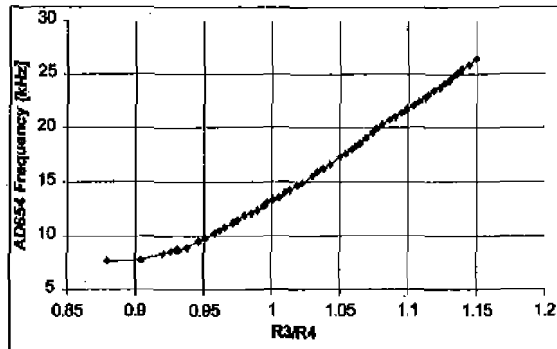

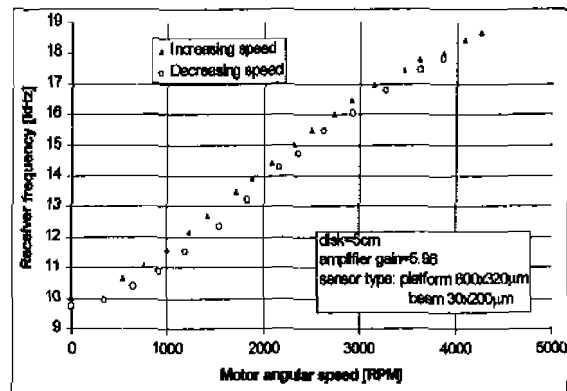*Figure 8. Schematic drawing of the transmition circuit system.*

Figure 9. Signal output of a micro-rotation sensor with signals transduced by a commercial wireless circuitry. The sensor tested in this case has a 600X320μm platform supported 30μm wide, 200μm long beams. The MCNC polysilicon beams are typically about 3μm thick.

4. CONCLUSION

The design of a novel surface-micromachined rotation sensor is presented. It is designed to detect the angular velocity of a rotating element by measuring the resistance change due to stress induced by centrifugal force on the seismic mass using piezoresistive effects. Likewise, based on theoreticl analysis, the angular acceleration and direction of rotation can also be estimated. The designed sensors were fabricated using the MUMPs 29 run. Several wireless transmission schemes for the rotation sensors were evaluated and we have selected the Radiometric transmission-receiving chips for our experiments. Experimental results showed a 15μg platform proof-mass could be used to detect rotation speeds of 1000 to 5000 rpm if appropriate structural designs are implemented by micro-machining technologies. Further testing (e.g., temperature and hysteresis) and calibration of the sensors will also be

accomplished in order to ensure the sensors give accurate and reliable data.

REFERENCES

1. J. A. Haslam, et al., Engineering instrumentation and control, 1993, pp. 133.
2. C. L. Nachtigal, Instrumentation and control – Fundamentals and Applications, 1990, pp. 370.
3. http://catalogue.pwallen.co.uk.
4. R. C. Spooncer, et al., "An optical tachometer with optical fibre links", IEE Colloquium on IREM, 1991.
5. T. A. Kwa, et al., "An integrated high-resolution optical angular displacement sensor" IEEE Transducers '91, pp. 368-371.
6. K. Watanabe, et al., "Non-contact revolution measurement by the magnetic field intensity from axes", IEEE IMTC '94, 2, pp. 605-608.
7. A. Powell, et al., "Optimisation of magnetic speed sensors", IEEE Trans. on Mag. '96, 32, pp. 4977-9.
8. T. Fabian, et al., "A robust capacitive angular speed sensor", IEEE IMTC '97, 2, pp. 1267-1272.
9. J. Soderkvist, "Piezoelectric beams and angular rate sensors", IEEE Proc. on the 44th Annual Symposium On Frequency Control, 1990.
10. A. M. Madni, et al., "A microelectromechanical quartz rotational rate sensor for inertial applications", IEEE Aeros. App. Conf., 1996, 2, pp. 315-332.
11. R. Voss, et al., "Silicon angular rate sensor for automotive applications with piezoelectric drive and piezoresistive read-out", IEEE TRANSDUCERS '97, 2, pp. 879-882.
12. L. S. Fan, et al., IEEE Trans. on Electron Devices, 1988, 35. pp. 724-730.
13. T. G. Beckwith, et al., Mechanical measurements, 3rd edition, 1982.
14. B. Kloeck, "Piezoresistive sensors", Sensors – A comprehensive survey, 1994, 7, pp. 158-163.
15. D. A. Koester, et al., SmartMUMPS Design Handbook including MUMPs introduction and Design Rules Rev. 4.0, MEMS Technology Applications Center, March 1996.
16. C. S. Smith, Phys. Rev. 94, 1954, pp. 42-49.
17. R. E. Beaty, et al., "Evaluation of Piezoresistive coefficient variation in silicon stress sensors using a four-point bending test fixture", IEEE Trans. on CHMT '92, 15, pp. 904-914.